

information can exchange between DG i and DG j if $(i, j) \in \mathcal{E}_C$. The Perron matrix of the graph \mathcal{G}_C [8] is defined as $W = \{w_{ij}\}$ with w_{ij} being the Metropolis weights, i.e.,

$$w_{ij} = \begin{cases} (1 + \max\{|\mathcal{N}_i|, |\mathcal{N}_j|\})^{-1}, & j \in \mathcal{N}_i \\ 1 - \sum_{s \in \mathcal{N}_i} w_{is}, & i = j \\ 0, & \text{others} \end{cases} \quad (3)$$

where $\mathcal{N}_i = \{j \in \mathcal{V}_C | (i, j) \in \mathcal{E}_C\}$ denotes the finite set of the neighbors of DG i 's distributed controller, and $|\mathcal{N}_i|$ denotes its cardinality, i.e., the number of neighbors of DG i .

C. Control Objectives

Two control objectives are considered in this study, i.e., the proportional active power sharing and frequency regulation [6], defined in the sequel.

Objective 1 (Proportional Active Power Sharing): The proportional active power sharing is achieved if the total active power demand is shared proportionally according to DGs' capacities P_i^{\max} in steady-state, i.e.,

$$P_i/P_i^{\max} = P_j/P_j^{\max}, \quad \forall i, j \in \mathcal{V}_E. \quad (4)$$

Objective 2 (Frequency Regulation): The frequency regulation is achieved if all the DGs' frequencies are equal to the nominal one in the steady-state, i.e.,

$$\omega_i = \omega_0, \quad \forall i \in \mathcal{V}_E. \quad (5)$$

In addition to the above two objectives, the privacy of the local information, i.e., the active power outputs and capacities of DGs [9], is required to be protected during the realization of these objectives.

III. ACTIVE POWER REFERENCE GENERATION

In this section, the control problem defined in Section II-C is transformed into an equivalent active power reference generation problem based on the global active power utilization level [1]. For a microgrid, the active power supply-demand balance can be expressed as

$$\sum_{i \in \mathcal{V}_E} P_i = P^{\text{Load}} + P^{\text{Loss}} \quad (6)$$

where P^{Load} and P^{Loss} are the load active power requirement and the total active power loss of the transmission lines. Thereafter, the global active power utilization level K^U can be defined as

$$K^U = \frac{P^{\text{Load}} + P^{\text{Loss}}}{\sum_{i \in \mathcal{V}_E} P_i^{\max}} = \frac{\sum_{i \in \mathcal{V}_E} P_i}{\sum_{i \in \mathcal{V}_E} P_i^{\max}}. \quad (7)$$

Moreover, select the active power references of the DGs' droop controllers as

$$P_i^{\text{ref}} = K^U P_i^{\max}. \quad (8)$$

Next, the active power outputs and frequencies of DGs in the steady-state are analyzed based on the droop control (1) with the active power references given by (8).

Taking the summations of both sides of (8) and substituting (7) into the resulting equation yield

$$\sum_{i \in \mathcal{V}_E} P_i^{\text{ref}} = \frac{\sum_{i \in \mathcal{V}_E} P_i}{\sum_{i \in \mathcal{V}_E} P_i^{\max}} \sum_{i \in \mathcal{V}_E} P_i^{\max} = \sum_{i \in \mathcal{V}_E} P_i. \quad (9)$$

Since all the DGs' frequencies are identical in the steady-state, i.e., $\omega_i = \omega_j, \forall i, j \in \mathcal{V}_E$, combining (1) and (9) yields

$$\begin{aligned} 0 &= \sum_{i \in \mathcal{V}_E} P_i^{\text{ref}} - \sum_{i \in \mathcal{V}_E} P_i = \sum_{i \in \mathcal{V}_E} (P_i^{\text{ref}} - P_i) \\ &= \sum_{i \in \mathcal{V}_E} m_i^{-1} (\omega_i - \omega_0) = (\omega_i - \omega_0) \sum_{i \in \mathcal{V}_E} m_i^{-1}. \end{aligned} \quad (10)$$

Considering the fact that the droop coefficients $m_i, \forall i \in \mathcal{V}_E$ are positive, one has $\sum_{i \in \mathcal{V}_E} m_i^{-1} > 0$. Then (10) becomes

$$\omega_i = \omega_0, \quad \forall i \in \mathcal{V}_E. \quad (11)$$

Hence, all DGs' frequencies are equal to the nominal value ω_0 in the steady-state.

Furthermore, combining (1), (8), and (11) gives

$$P_i/P_i^{\max} = P_i^{\text{ref}}/P_i^{\max} = K^U, \quad \forall i \in \mathcal{V}_E. \quad (12)$$

Therefore, the ratios of all DGs' active outputs to their capacities are identical to the global utilization level.

From the above steady-state results given by (11) and (12), it can be noticed that if the global utilization level K^U is known to all DGs, then the control objectives can be achieved simply by selecting the active power references of the droop control by (8). However, K^U is a global variable whose calculation requires all the active power outputs and capacities of DGs and a centralized communication network. Besides, the privacy of these sensitive data is jeopardized. To address these issues, a PPC algorithm is presented in the next section to obtain the global K^U in a distributed manner with preserved privacy.

IV. PPC-BASED DISTRIBUTED CONTROL

In this section, a PPC algorithm is presented to accurately obtain the global utilization level K^U which is further used to update the active power references by (8) and achieve the control objectives. Firstly, rewrite (7) as

$$K^U = \frac{\sum_{i \in \mathcal{V}_E} P_i/N}{\sum_{i \in \mathcal{V}_E} P_i^{\max}/N}. \quad (13)$$

Since the numerator and denominator are the average values of the DGs' active power outputs and capacities, respectively, they can be obtained through the traditional average consensus algorithm [8].

For clarity, define two states, \bar{P}_i and \bar{P}_i^{\max} , for DG $i, i \in \mathcal{V}_E$. Let $\bar{P}_i(0)$ and $\bar{P}_i^{\max}(0)$ be the actual sampled active power output and capacity data, respectively. Further, denote $\bar{P}_i(k)$ and $\bar{P}_i^{\max}(k)$ as the states of DG i at periodic discrete-time instants $t = kT_C, k = 0, 1, 2, \dots$, where T_C is the communication period for the distributed controllers. Notice that only the data $\bar{P}_i(0)$ and $\bar{P}_i^{\max}(0)$ are sensitive and should be protected since they contain the actual information of DGs.

For brevity, only the acquirement of the numerator $\sum_{i \in \mathcal{V}_E} P_i/N$ is presented in detail, and that of the denominator is similar and therefore omitted here. According to [8], the traditional consensus algorithm can be expressed as

$$\bar{P}_i(k+1) = w_{ii}\bar{P}_i(k) + \sum_{j \in \mathcal{N}_i} w_{ij}\bar{P}_j(k). \quad (14)$$

Notice that at $k = 0$, the actual active power output data $P_j = P_j(0)$ of DG $j, j \in \mathcal{N}_i$ is directly transmitted to its neighbor DG i . To protect the sensitive data $\bar{P}_i(0)$, a random

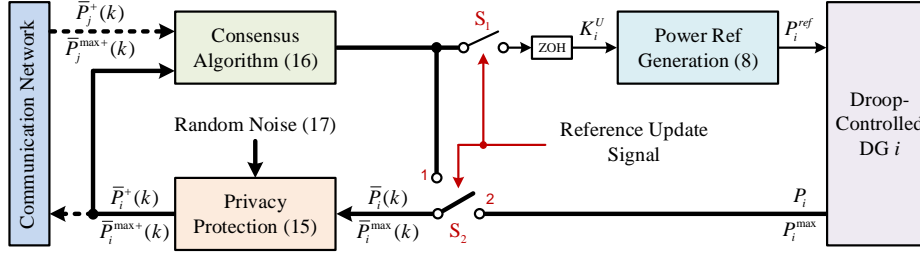


Fig. 2. Diagram of the proposed PPC-based distributed controller.

noise $d_i(k)$ is added to the sensitive data before it is sent to its neighbor DGs as follows

$$\bar{P}_i^+(k) = \bar{P}_i(k) + d_i(k). \quad (15)$$

The PPC algorithm is then given as

$$\bar{P}_i(k+1) = w_{ii}\bar{P}_i^+(k) + \sum_{j \in \mathcal{N}_i} w_{ij}\bar{P}_j^+(k). \quad (16)$$

As analyzed in Section III, to achieve the control objectives, the accurate value of the utilization level K^U is required, i.e., the accurate average values of the active power outputs and capacities are required. For this purpose, the random noise for DG i , $i \in \mathcal{V}_E$ can be generated locally by

$$d_i(k) = \begin{cases} r_i(k), & k = 0 \\ r_i(k) - r_i(k-1), & \text{others} \end{cases} \quad (17)$$

where $r_i(k)$ is a random number selected from $[-\alpha\rho^{k+1}, \alpha\rho^{k+1}]$ at each iteration k with $\alpha > 0$ and $0 \leq \rho < 1$. According to [10, Corollary 3.2], all the states \bar{P}_i can converge to the average of their initial values accurately, i.e., $\bar{P}_i(\infty) = \sum_{i \in \mathcal{V}_E} \bar{P}_i(0)/N$, $i \in \mathcal{V}_E$.

Notice that $\bar{P}_i(0)$ is equal to the actual active power output P_i . Hence, $\bar{P}_i(\infty) = \sum_{i \in \mathcal{V}_E} P_i/N$. The average value of the DGs' active power outputs is obtained in a distributed manner with preserved privacy. Similarly, with the PPC algorithm, the average value of the DGs' active power capacities can be attained, i.e., $\bar{P}_i^{\max}(\infty) = \sum_{i \in \mathcal{V}_E} P_i^{\max}/N$. Then the local utilization level can be calculated as

$$K_i^U = \frac{\bar{P}_i(\infty)}{\bar{P}_i^{\max}(\infty)} = \frac{\sum_{i \in \mathcal{V}_E} P_i/N}{\sum_{i \in \mathcal{V}_E} P_i^{\max}/N} = K^U. \quad (18)$$

Thus, the global utilization level K^U can be acquired accurately through (16) with preserved privacy.

Remark 1 (Privacy Analysis): The PPC algorithm can achieve the (ϵ, σ) -data-privacy [10, Theorem 3.9], i.e., $\Pr\{|\hat{P}_i - P_i| \leq \epsilon\} \leq \sigma$ with $\sigma = \max_{|\nu| \leq \alpha\rho} \int_{\nu-\epsilon}^{\nu+\epsilon} f_{d_i(0)}(x)dx$ where \hat{P}_i is the estimate of P_i , and $f_{d_i(0)}$ is the probability density function of $d_i(0)$. Hence, the probability of the accurate estimate of P_i is 0 since $\lim_{\epsilon \rightarrow 0} \sigma = 0$. More specifically, the actual information of active power outputs of all DGs can be protected during the discovery process of K^U . Moreover, with a similar process, the information of actual active power capacities of all DGs can also be protected.

A. Control Implementation

The control diagram of the proposed PPC-based distributed control design is given in Fig. 2.

Firstly, a reference update triggering signal is generated for the microgrid, which is triggered at periodic discrete-time instants $t = 0, T_U, 2T_U, \dots$ with T_U being the reference updating period. In this study, T_U is selected as $T_U = k^{\max}T_C$ where k^{\max} is the maximum iteration number that can guarantee the convergence of the consensus algorithm.

When the reference update signal is triggered, S_1 is closed and S_2 is switched to "2". The outputs of the consensus algorithm, i.e., the average values of the DGs' active power outputs and capacities, are used to calculate the local utilization level K_i^U through (18). Then the active power references are updated by (8). Besides, the actual active power output P_i and capacity P_i^{\max} are sampled. To prepare for the next utilization level update, set $k = 0$, $\bar{P}_i(0) = P_i$, and $\bar{P}_i^{\max}(0) = P_i^{\max}$ for the consensus algorithm (16) and the random noise (17).

When the reference update signal is released, S_1 is open and S_2 is switched to "1". The local utilization level K_i^U is maintained unchanged through a zero-order-hold module. The PPC algorithm (16) is implemented to generate a new utilization level K_i^U for the next updating period.

Notice that all data being transmitted through the communication network is protected through the privacy protection module with noise added as described in (17).

Remark 2 (Constant Power Capacity): For constant active power capacities for DGs [7], their average value can be obtained through running the PPC algorithm once and kept unchanged afterward to reduce communication times and avoid possible privacy leakage.

Remark 3 (P_i^{\max} -Independent Droop Coefficient): The total active power demand is traditionally shared among the DGs according to their capacity-dependent droop coefficients m_i . In this study, the total active power demand is shared independently of m_i since $\omega_i = \omega_0$ and $P_i = P_i^{ref}$ as discussed in Section III. Such a feature allows the selection of m_i independently of the capacity P_i^{\max} .

V. VERIFICATION STUDIES

The performance of the proposed controller is tested with a switch-level microgrid model illustrated in Fig. 1. The system and control parameters are listed in Table I where $Z_b = R_b + j\omega L_b$ with $R_b = 0.1 \Omega$, $L_b = 1$ mH. Two 5 kW resistive loads are connected to the system at 0.2 s and 0.6 s, respectively, and disconnected at 1 s and 1.4 s afterward.

The corresponding results are shown in Figs. 3-6. From Figs. 4 and 5, one can notice that when the DGs' active power references update at 0.4 s, 0.8 s, 1.2 s, and 1.6 s, the DGs' frequencies can restore to the nominal value. Also, as shown in

TABLE I
MICROGRID SYSTEM AND CONTROL PARAMETERS

Quantity	Value
Transmission line Z_i (Ω)	$2Z^b, 3Z^b, Z^b, 4Z^b$
Nominal frequency (Hz)	50
Nominal voltage (V)	311
Nominal power (kW)	10
DG's capacity P_i^{\max} (p.u.)	0.4, 0.3, 0.2, 0.1
Power filter bandwidth (Hz)	10
Carrier frequency (kHz)	10
Communication period T_C (ms)	4
Reference updating period T_U (ms)	100
Droop coefficient m_i (10^{-4})	1.57, 2.09, 3.14, 6.28
Droop coefficient n_i (10^{-3})	0.778, 1.04, 1.56, 3.11
Metropolis weight $w_{12}, w_{23}, w_{34}, w_{41}$	1/3
Noise parameter α, ρ	5000, 0.6

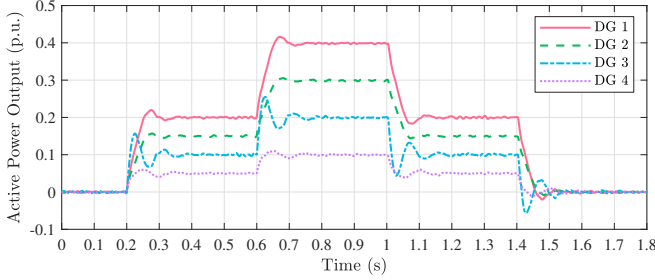


Fig. 3. Active power outputs P_i of DGs.

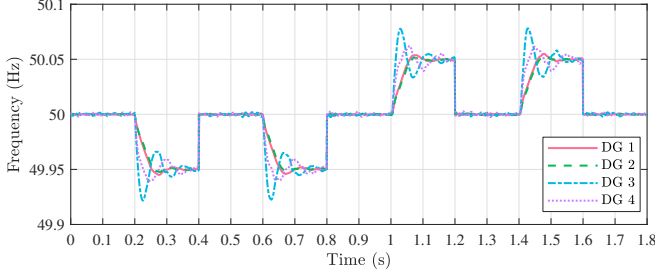


Fig. 4. Frequencies $\omega_i/2\pi$ of DGs.

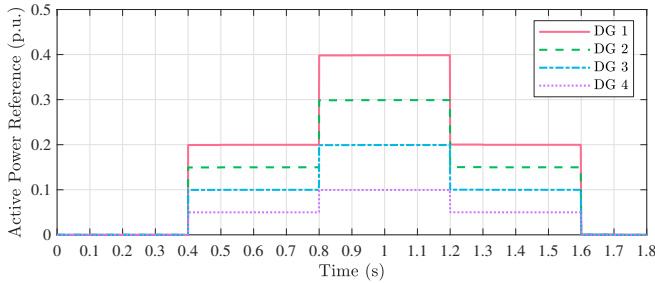


Fig. 5. Active power references P_i^{ref} of DGs.

Fig. 3, the proportional active power sharing is also achieved. Finally, Fig. 6 illustrates the comparison results between the sampled power outputs and the power outputs with noise. One can see that the transmitted data are totally different from their original ones in both the power outputs and their trends. The privacy of this sensitive information is thus protected.

VI. CONCLUSION

This letter presents a PPC-based algorithm to achieve active power sharing and frequency regulation in microgrids. By taking the virtue of the global utilization level, the original

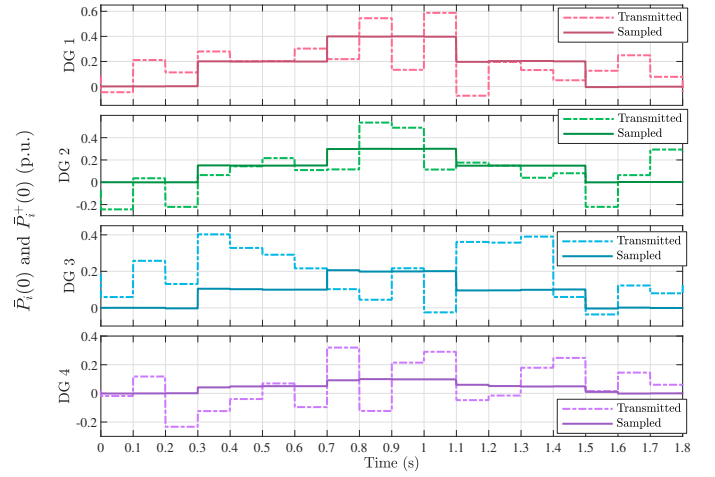


Fig. 6. Comparison between the sampled power outputs $\bar{P}_i(0)$ and the transmitted power outputs with noise $\bar{P}_i^+(0)$.

control problem is transformed into an equivalent active power reference generation problem. Thereafter, a PPC-based algorithm is presented to obtain the global utilization level in a distributed manner with *preserved privacy*. Finally, verification studies on a switch-level microgrid with four DGs are carried out to showcase the effectiveness of the proposed approach.

REFERENCES

- [1] B. Fan, J. Peng, J. Duan, Q. Yang, and W. Liu, "Distributed control of multiple-bus microgrid with paralleled distributed generators," *IEEE/CAA Journal of Automatica Sinica*, vol. 6, no. 3, pp. 676–684, 2019.
- [2] Y. Khayat, Q. Shafiee, R. Heydari, M. Naderi, T. Dragičević, J. W. Simpson-Porco, F. Dörfler, M. Fathi, F. Blaabjerg, J. M. Guerrero *et al.*, "On the secondary control architectures of AC microgrids: An overview," *IEEE Transactions on Power Electronics*, vol. 35, no. 6, pp. 6482–6500, 2020.
- [3] M. Eskandari, L. Li, M. H. Moradi, P. Siano, and F. Blaabjerg, "Active power sharing and frequency restoration in an autonomous networked microgrid," *IEEE Transactions on Power Systems*, vol. 34, no. 6, pp. 4706–4717, 2019.
- [4] M. Awal, H. Yu, H. Tu, S. M. Lukic, and I. Husain, "Hierarchical control for virtual oscillator based grid-connected and islanded microgrids," *IEEE Transactions on Power Electronics*, vol. 35, no. 1, pp. 988–1001, 2020.
- [5] S. Weng, D. Yue, C. Dou, J. Shi, and C. Huang, "Distributed event-triggered cooperative control for frequency and voltage stability and power sharing in isolated inverter-based microgrid," *IEEE Transactions on Cybernetics*, vol. 49, no. 4, pp. 1427–1439, 2019.
- [6] L. Ding, Q.-L. Han, and X.-M. Zhang, "Distributed secondary control for active power sharing and frequency regulation in islanded microgrids using an event-triggered communication mechanism," *IEEE Transactions on Industrial Informatics*, vol. 15, no. 7, pp. 3910–3922, 2019.
- [7] J. Lai, X. Lu, and X. Yu, "Stochastic distributed frequency and load sharing control for microgrids with communication delays," *IEEE Systems Journal*, vol. 13, no. 4, pp. 4269–4280, 2019.
- [8] R. Olfati-Saber, J. A. Fax, and R. M. Murray, "Consensus and cooperation in networked multi-agent systems," *Proceedings of the IEEE*, vol. 95, no. 1, pp. 215–233, 2007.
- [9] Q. Zhou, M. Shahidehpour, A. Abdulwhab, and A. M. Abusorrah, "Privacy-preserving distributed control strategy for optimal economic operation in islanded reconfigurable microgrids," *IEEE Transactions on Power Systems*, vol. 35, no. 5, pp. 3847–3856, 2020.
- [10] J. He, L. Cai, P. Cheng, J. Pan, and L. Shi, "Consensus-based data-privacy preserving data aggregation," *IEEE Transactions on Automatic Control*, vol. 64, no. 12, pp. 5222–5229, 2019.